Hindawi Publishing Corporation
International Journal of Manufacturing Engineering
Volume 2014, Article ID 154784, 6 pages
http://dx.doi.org/10.1155/2014/154784

Research Article

Resistance Spot Welding Optimization Based on Artificial Neural Network

Thongchai Arunchai,[1] Kawin Sonthipermpoon,[1] Phisut Apichayakul,[1] and Kreangsak Tamee[2]

[1] *Department of Industrial Engineering, Faculty of Engineering, Naresuan University, Phitsanulok 65000, Thailand*
[2] *Department of Computer Science and Information Technology, Faculty of Science, Naresuan University, Phitsanulok 65000, Thailand*

Correspondence should be addressed to Thongchai Arunchai; t_ch@hotmail.com

Received 15 August 2014; Accepted 19 October 2014; Published 9 November 2014

Academic Editor: Quanfang Chen

Resistance Spot Welding (RSW) is processed by using aluminum alloy used in the automotive industry. The difficulty of RSW parameter setting leads to inconsistent quality between welds. The important RSW parameters are the welding current, electrode force, and welding time. An additional RSW parameter, that is, the electrical resistance of the aluminum alloy, which varies depending on the thickness of the material, is considered to be a necessary parameter. The parameters applied to the RSW process, with aluminum alloy, are sensitive to exact measurement. Parameter prediction by the use of an artificial neural network (ANN) as a tool in finding the parameter optimization was investigated. The ANN was designed and tested for predictive weld quality by using the input and output data in parameters and tensile shear strength of the aluminum alloy, respectively. The results of the tensile shear strength testing and the estimated parameter optimization are applied to the RSW process. The achieved results of the tensile shear strength output were mean squared error (MSE) and accuracy equal to 0.054 and 95%, respectively. This indicates that that the application of the ANN in welding machine control is highly successful in setting the welding parameters.

1. Introduction

In automotive production, each automobile has approximately 7,000 to 12,000 spot welds. The welds are done using the Resistance Spot Welding (RSW) process which is done by a computer controlled robotic welder. The use of RSW on lightweight aluminum alloy is increasing [1, 2]. RSW is a rapid joining technique extensively used to join thin shell assemblies in automotive manufacturing operations. It is an important process to ensure strong structural car bodies using lightweight materials to save both energy and natural resources [3]. The aluminum alloy material is a low density material with significant mechanical properties which is expected to be extensively used in the future to partially replace steel which is currently the primary production material in automobiles [4]. The 6061-T6 aluminum alloy is of light weight and has significant mechanical properties which are of interest in this research.

The weld quality of the RSW process has been a significant problem for the automotive industry. Manual calculation of welding parameters, operator experience, and technician expertise in adjusting the parameter settings have not been consistently accurate or correct. The calculations have previously been unable to be confirmed against optimal parameters [5]. The parameter settings of each welding machine have been difficult because there are many sensitive factors. This has led to the high cost of requiring many specimens of the construction material to be tested to achieve adequate experimental results to derive optimal parameter values. Each car body factory has more than 200 welding machines. In order to get standard weld quality overall has led to high costs of adjusting the parameter settings for each different model of welding machine, for different materials (e.g., thickness), for replacement electrodes, and so on [6–8]. Therefore, it is important to understand the parameter relationships in the RSW process, quality improvement measures, assessment

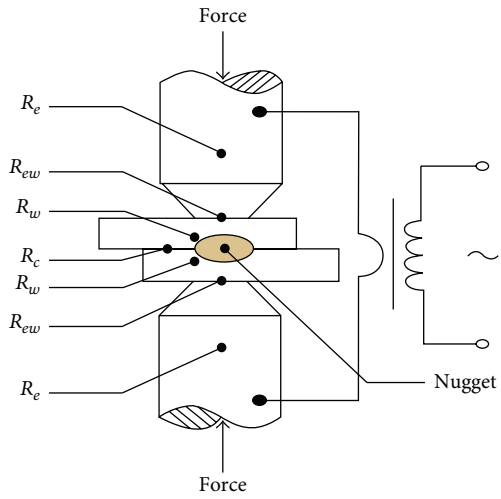

FIGURE 1: The resistance in RSW process [10].

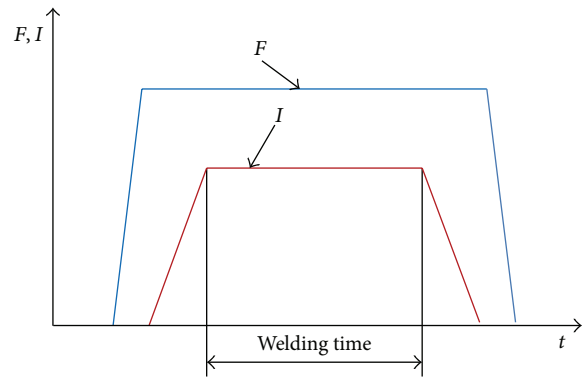

FIGURE 2: RSW schematic diagram.

and efficiency prediction, and appropriate parameter optimization.

The problems mentioned have motivated this study, formally titled "parameter optimization for resistance spot welding of 6061-T6 aluminum alloy based on artificial neural network." The estimation of RSW parameters using ANN will be more efficiently and correctly optimized. The ANN proved to be effective in resolving both linear and nonlinear functions required for adjusting the RSW parameter settings of computer controlled robotic welders, especially in the automotive industry.

2. RSW Process

The objective of the RSW process is to generate heat rapidly in the joints of the material being welded while minimizing conduction of heat to cooler adjacent material. This heat generation can be expressed by

$$Q = I^2Rt, \tag{1}$$

where Q is the heat energy in joules, I is the current in amperes, R is the resistance in ohms, and t is the time in seconds [9]. The series of resistances contributed by the secondary circuit resistance welding machine are shown in Figure 1.

From Figure 1, the resistance in the RSW process depends on the total resistance which can be expressed by

$$R = R_c + 2R_w + 2R_{ew} + 2R_e, \tag{2}$$

where R is the total resistance, R_e is the electrode resistance, R_{ew} is the specimen electrode contact resistance, R_w is the specimen resistance, and R_c is the specimen's contact resistance.

The resistance transformation of the material work piece affects the melting temperature in the spot weld in the RSW process and the weld ability of the material [11, 12]. Optimal electrode force is needed for the explosive solutions during material smelting [13, 14], while the intensity of the electric welding current is an important factor that affects heat generation leading to smelting. When the electric intensity is high the spot weld will also have intensive heat. This will affect the nugget size and strength of the weld joint [15]. The nugget size and weld joint strength depend on the resistance and welding time, so the welding duration influences the mechanical properties of the weld joints [16, 17]. Melting occurs as a result of the relationship between welding current, welding time, and electrode force, as shown in schematic diagram RSW cycle Figure 2, where I is welding current, t is welding time, and F is electrode force.

Researchers have studied the relationship of the RSW parameters and confirm that the welding process parameters have a great influence on the weld quality [18, 19]. In addition, the resistance of the material due to the thickness of the work piece is also important, as can be seen in greater nugget growth in thicker pieces than thin pieces. In different materials, a satisfactory nugget will be generated in high resistance materials or materials with lower thermal conductivity [20]. Therefore, this study adds the resistance as a factor.

3. Material and Methods

This research studied the RSW process under actual conditions in a car body factory which used gun welds controlled by a MFDC Rexroth Bosch welder. Aluminum alloy specimens (6061-T6) of both 1 and 2 mm thickness were welded at three resistance levels. Figure 3 shows the three resistance levels of the high, medium, and low thicknesses of 2-2, 2-1, and 1-1 mm material, respectively.

The mechanical and chemical properties based on KAISER ALUMINUM [21] are shown in Tables 1 and 2, respectively.

This research used 6 mm copper alloy electrode tips. The experimental design included full factorial analysis based on low, medium, and high thickness of material, with all parameter settings varied at each level of thickness, giving $3^4 \times 3 = 243$ runs. The parameter settings are welding current,

Table 1: 6061-T6 aluminum alloy chemical properties.

6061	Si	Fe	Cu	Mn	Mg	Cr	Zn	Ti	Zr	Other	Max.
Min. (wt%)	0.40	0.0	0.15	0.00	0.8	0.04	0.00	0.00	0.00	Each	0.05
Max. (wt%)	0.8	0.7	0.40	0.15	1.2	0.35	0.25	0.15	0.05	Total	0.15

Table 2: 6061-T6 aluminum alloy mechanical properties.

	Temper T6		
Tensile tests	Ultimate (MPA)	Yield (MPA)	Elongation (%)
Min.: Max.	337 : 340	286 : 288	13.6 : 13.9

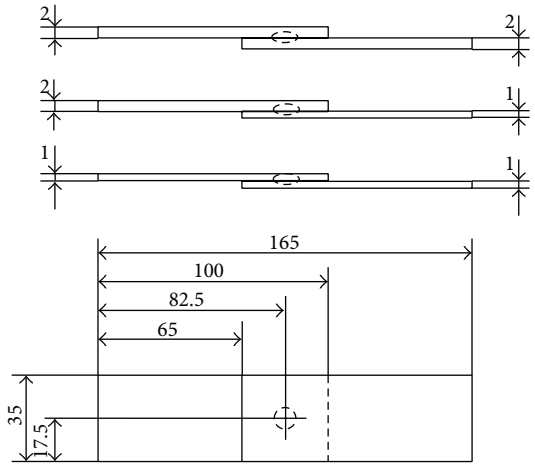

Figure 3: The specimen dimensions (mm).

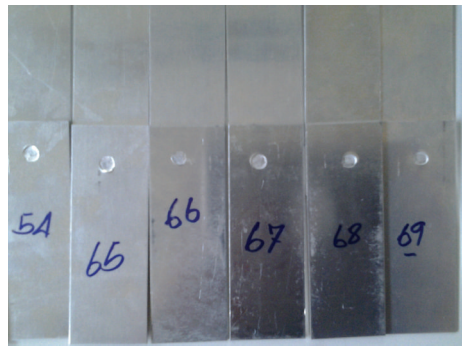

(a)

(b)

(c)

Figure 4: (a) is the weld joint, (b) is the tested clamping, and (c) is the graphic monitor.

electrode force, welding time, and resistance of 20, 28, and 36 kA, 2, 4, and 6 kN, 100, 150, and 200 ms and 2-2, 2-1, and 1-1 mm, respectively. Subsequently the welding parameters were input according to the experimental design and welding tests were done. The finished weld joints and the maximum tensile shear strength were tested and recorded. The tests were done using the HOUNSFIELD 50 kN at maximum load as shown in Figure 4.

In this research, 75% of the 243 experimental results of the ANN were used to train the robotic welders. 25% of the experimental results were selected randomly for testing, for comparison between the predicted shear strength and the experimental shear strength results. The ANN models were configured to establish the relationship between the welding parameters and the shear strength. The ANN model is a multilayered feed-forward algorithm, as shown in Figure 5. In that algorithm, there are three layers: the input layer, the output layer, and the hidden layer between the input and output layers. In the input layer, the number of the input neurons is set to the level of welding parameters in each run order, and the output layer is the shear strength.

The ANN was designed and tested for estimating the shear strength by using the welding parameters as input data and the shear strength as output data, using the multilayered feed-forward algorithm, and the ANN was trained by the backpropagation algorithm. The final transfer function was a sigmoidal function and was a pure linear function.

4. Results and Discussion

This work studied the application of the ANN to calculate optimized parameters for controlling welding robots. Table 3 shows the tensile shear strength achieved from actual application of the experimental results as calculated by the ANN; this variable is the calculation of the mean squared error (MSE) of the shear strength. The MSE is equal to 0.05. According to these results, it can be seen that the ANN determined appropriate parameter optimization with satisfactory results.

The shear strength is obtained when applying the experimental results from the ANN. Applying the ANN calculations results in good parameter optimization as shown in Figure 6.

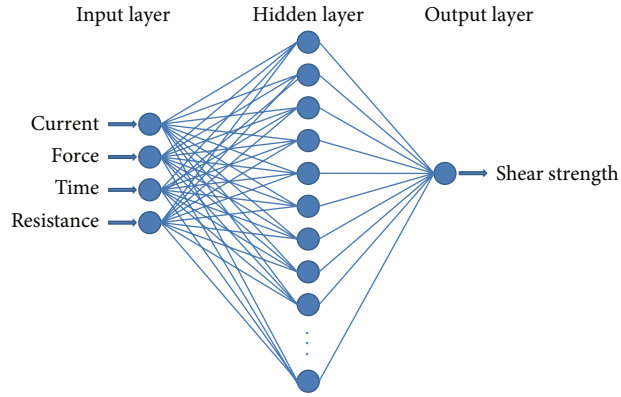

Figure 5: The ANN structure for shear strength prediction.

Table 3: Show calculation of the mean squared error (MSE).

Number	Shear strength (kN)	ANN prediction	Squared error	Number	Shear strength (kN)	ANN prediction	Squared error	Number	Shear strength (kN)	ANN prediction	Squared error
1	1.92	2.0571	0.018796	21	3.585	3.669	0.007056	41	3.271	3.3765	0.01113
2	3.11	3.1568	0.00219	22	1.985	2.0526	0.00457	42	3.623	3.76	0.018769
3	2.695	2.293	0.161604	23	3.611	3.6838	0.0053	43	3.447	3.6838	0.056074
4	2.505	2.3748	0.016952	24	2.892	3.1432	0.063101	44	1.92	2.0571	0.018796
5	3.598	3.8369	0.057073	25	3.585	3.669	0.007056	45	1.842	1.9775	0.01836
6	2.558	2.4952	0.003944	26	2.84	3.1568	0.100362	46	3.802	3.9422	0.019656
7	3.271	3.3765	0.01113	27	3.623	3.76	0.018769	47	3.836	3.8369	$8.1E-07$
8	3.485	3.0774	0.166138	28	2.662	2.6579	$1.68E-05$	48	1.963	2.1044	0.019994
9	3.505	3.592	0.007569	29	3.572	2.9412	0.397909	49	2.816	3.1432	0.10706
10	1.882	2.3376	0.207571	30	1.89	1.9507	0.003684	50	2.866	2.9608	0.008987
11	2.405	2.9412	0.28751	31	3.566	3.592	0.000676	51	1.884	2.0143	0.016978
12	3.458	3.669	0.044521	32	3.185	3.1284	0.003204	52	2.843	2.6913	0.023013
13	3.848	3.8369	0.000123	33	3.84	3.9422	0.010445	53	2.708	2.6617	0.002144
14	3.878	3.9422	0.004122	34	2.852	2.4274	0.180285	54	3.314	3.3765	0.003906
15	2.468	2.5167	0.002372	35	3.525	3.592	0.004489	55	3.235	2.6829	0.304814
16	3.316	3.1432	0.02986	36	3.626	3.6838	0.003341	56	3.285	3.1568	0.016435
17	2.865	2.5445	0.10272	37	1.942	2.1044	0.026374	57	2.837	2.6913	0.021228
18	1.99	2.1174	0.016231	38	3.066	3.1284	0.003894	58	2.702	2.8238	0.014835
19	2.883	2.8238	0.003505	39	2.861	3.1284	0.071503	59	3.485	3.0774	0.166138
20	2.685	2.5167	0.028325	40	3.623	3.76	0.018769	60	2.84	2.304	0.287296
MSE = 0.053978											

ANN is therefore seen as an appropriate method optimization for finding an answer that is both linear and nonlinear.

The ANN model is composed of three different layers: input layer, hidden layer, and output layer. The ANN was used to calculate the shear strength at the output layer and the RSW parameters at the input layer while training and using the backpropagation algorithm. 75% of the 243 data values from the full factorial experimental results were used for training and 25% of the data were used for testing the accuracy of the ANN's calculated values. The results show that hidden nodes, learning rate, MSE goal, and maximum learning epoch are 30, 0.001, 0.04, and 3,000,000, respectively.

When tested, 20 samples were found to have a mean squared error (MSE) of 0.047896 kN. This indicates that the ANN model is capable of predicting the shear strength for adjusting the RSW parameters under test with a small sample which are shown in Table 4 and Figure 7, respectively.

From this study, it is suggested that the RSW operator can use a small sample set appropriate as input into the ANN model which would be sufficient for setting the optimization

Table 4: Calculation of the mean squared error (MSE) case of 20-unit experiment.

Number	Shear strength (kN)	ANN prediction	Squared error	Number	Shear strength (kN)	ANN prediction	Squared error	Number	Shear strength (kN)	ANN prediction	Squared error
1	3.598	3.8369	0.057073	8	3.611	3.6838	0.0053	15	3.626	3.6838	0.003341
2	3.485	3.0774	0.166138	9	3.585	3.669	0.007056	16	3.623	3.76	0.018769
3	3.505	3.592	0.007569	10	3.623	3.76	0.018769	17	3.623	3.76	0.018769
4	3.458	3.669	0.044521	11	3.572	2.9412	0.397909	18	3.802	3.9422	0.019656
5	3.848	3.8369	0.000123	12	3.566	3.592	0.000676	19	3.836	3.8369	0.000000
6	3.878	3.9422	0.004122	13	3.84	3.9422	0.010445	20	3.485	3.0774	0.166138
7	3.585	3.669	0.007056	14	3.525	3.592	0.004489				
MSE = 0.047896											

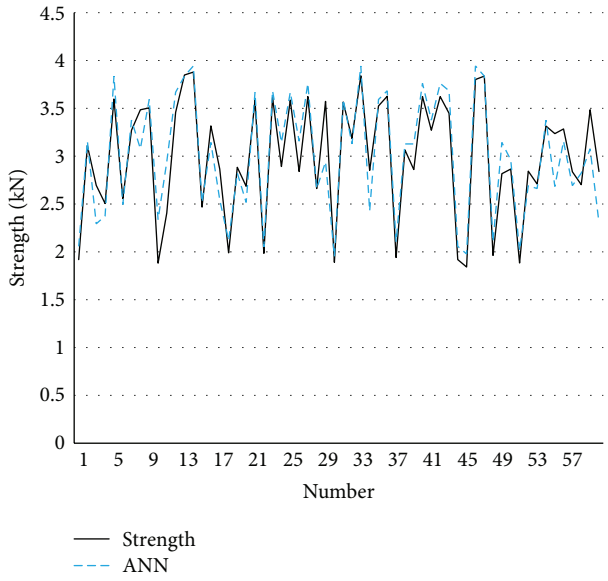

Figure 6: ANN prediction.

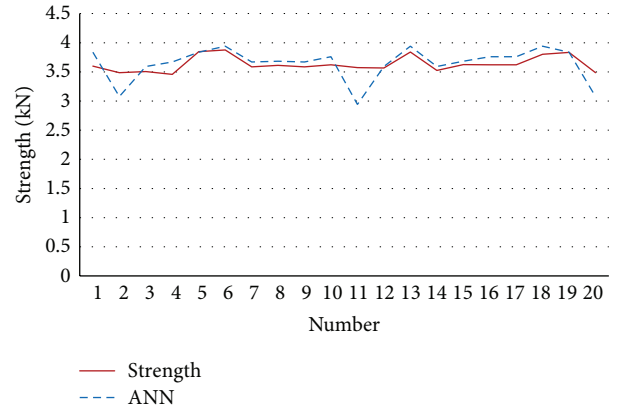

Figure 7: ANN prediction case of 20-unit experiment.

parameters. However, the accuracy of the parameters may be affected by other factors outside the scope of the ANN, such as the particular welding machine model, the surface condition of the specimen material, the cooling effect of the environment, and electrode wear.

5. Conclusion

The full factorial experimental results and ANN were developed and successfully tested in an auto body industry plant in Thailand. The results were MSE and accuracy equal to 0.054 and 95%, respectively. Calculating a reliable estimation of shear strength enables parameter settings to achieve high weld quality and reduces both the setting time process and the sample testing. Future work should test the accuracy of other algorithms used to calculate these parameters to enable comparison of the accuracy of other algorithms.

Conflict of Interests

The authors declare that there is no conflict of interests regarding the publication of this paper.

Acknowledgments

The authors would like to express their profound gratitude to the UK Engineering and Supply Co. Ltd. and Thonburi Automotive Assembly Plant Co., Ltd., Thailand, for allowing use of their premises and providing research equipment to support the project.

References

[1] H. Huh and W. Kang, "Electrothermal analysis of electric resistance spot welding processes by a 3-D finite element method," *Journal of Materials Processing Technology*, vol. 63, no. 1–3, pp. 672–677, 1997.

[2] W. Li, S. Cheng, S. J. Hu, and J. Shriver, "Statistical investigation on resistance spot welding quality using a two-state, sliding-level experiment," *Journal of Manufacturing Science and Engineering, Transactions of the ASME*, vol. 123, no. 3, pp. 513–520, 2001.

[3] J. A. Khan, L. Xu, Y.-J. Chao, and K. Broach, "Numerical simulation of resistance spot welding process," *Numerical Heat Transfer Part A: Applications*, vol. 37, no. 5, pp. 425–446, 2000.

[4] J. Zhu, L. Li, and Z. Liu, "CO_2 and diode laser welding of AZ31 magnesium alloy," *Applied Surface Science*, vol. 247, no. 1–4, pp. 300–306, 2005.

[5] H.-L. Lin, T. Chou, and C.-P. Chou, "Optimation of resistance spot welding process using Taguchi method and a neural network," *Experimental Techniques*, vol. 31, no. 5, pp. 30–36, 2007.

[6] K. D. Weiss, "Paint and coatings: a mature industry in transition," *Progress in Polymer Science*, vol. 22, no. 2, pp. 203–245, 1997.

[7] X. Deng, W. Chen, and G. Shi, "Three-dimensional finite element analysis of the mechanical behavior of spot welds," *Finite Elements in Analysis and Design*, vol. 35, no. 1, pp. 17–39, 2000.

[8] S.-H. Lin, J. Pan, T. Tyan, and P. Prasad, "A general failure criterion for spot welds under combined loading conditions," *International Journal of Solids and Structures*, vol. 40, no. 21, pp. 5539–5564, 2003.

[9] N. T. Williams and J. D. Parker, "Review of resistance spot welding of steel sheets: part 2—factors influencing electrode life," *International Materials Reviews*, vol. 49, no. 2, pp. 77–108, 2004.

[10] Y. Luo, J. Liu, H. Xu, C. Xiong, and L. Liu, "Regression modeling and process analysis of resistance spot welding on galvanized steel sheet," *Materials and Design*, vol. 30, no. 7, pp. 2547–2555, 2009.

[11] P. H. Thornton, A. R. Krause, and R. G. Davies, "Contact resistances in spot welding," *Welding Journal*, vol. 75, no. 12, pp. 402.s–412.s, 1996.

[12] A. G. Livshits, "Universal quality assurance method for resistance spot welding based on dynamic resistance," *Welding Journal*, vol. 76, no. 9, pp. 383–390, 1997.

[13] R. B. Hirsch, "Making resistance spot welding safer," *Welding Journal*, vol. 86, no. 2, pp. 32–37, 2007.

[14] J. Senkara, H. Zhang, and S. J. Hu, "Expulsion prediction in resistance spot welding," *Welding Journal*, vol. 83, no. 4, p. 123-S, 2004.

[15] S. Satonaka, K. Kaieda, and S. Okamoto, "Prediction of tensile-shear strength of spot welds based on fracture modes," *Welding in the World*, vol. 48, no. 5-6, pp. 39–45, 2004.

[16] S. Aslanlar, A. Ogur, U. Ozsarac, and E. Ilhan, "Welding time effect on mechanical properties of automotive sheets in electrical resistance spot welding," *Materials and Design*, vol. 29, no. 7, pp. 1427–1431, 2008.

[17] F. Hayat, "The effects of the welding current on heat input, nugget geometry, and the mechanical and fractural properties of resistance spot welding on Mg/Al dissimilar materials," *Materials and Design*, vol. 32, no. 4, pp. 2476–2484, 2011.

[18] T. Kim, H. Park, and S. Rhee, "Optimization of welding parameters for resistance spot welding of TRIP steel with response surface methodology," *International Journal of Production Research*, vol. 43, no. 21, pp. 4643–4657, 2005.

[19] R. S. Florea, D. J. Bammann, A. Yeldell, K. N. Solanki, and Y. Hammi, "Welding parameters influence on fatigue life and microstructure in resistance spot welding of 6061-T6 aluminum alloy," *Materials and Design*, vol. 45, pp. 456–465, 2013.

[20] C. Tsai and J. Papritan, "Modeling of resistance spot weld nugget growth," *Welding Journal*, vol. 71, no. 2, pp. 47–54, 1992.

[21] KAISER ALUMINUM, "Trent wood Works—WA 99215 CERTIFIED Serial Number 4315467," Article ID 4315467, TEST REPORT, December 2013.